Optics Communications 344 (2015) 139–146

Contents lists available at ScienceDirect

Optics Communications

journal homepage: www.elsevier.com/locate/optcom

Optical frequency comb generation based on chirping of Mach–Zehnder Modulators

Jassim K. Hmood [a,b], Siamak D. Emami [a], Kamarul A. Noordin [a], Harith Ahmad [c], Sulaiman W. Harun [a,c,*], Hossam M.H. Shalaby [d]

[a] Department of Electrical Engineering, Faculty of Engineering, University of Malaya, 50603 Kuala Lumpur, Malaysia
[b] Laser and Optoelectronic Department, University of Technology, Baghdad 10066, Iraq
[c] Photonics Research Center, University of Malaya, Kuala Lumpur 50603, Malaysia
[d] Department of Electronics and Communications Engineering, Egypt-Japan University of Science and Technology, Alexandria 21934, Egypt

ARTICLE INFO

Article history:
Received 14 November 2014
Received in revised form
15 January 2015
Accepted 19 January 2015
Available online 21 January 2015

Keywords:
Chirp factor
Optical frequency comb
Optical fiber communication
Optical modulator

ABSTRACT

A new approach for the generation of an optical frequency comb, based on chirping of modulators, is proposed and numerically demonstrated. The setup includes two cascaded Mach–Zehnder Modulators (MZMs), a sinusoidal wave oscillator, and an electrical time delay. The first MZM is driven directly by a sinusoidal wave, while the second MZM is driven by a delayed replica of the sinusoidal wave. A mathematical model of the proposed system is formulated and modeled using the Matlab software. It is shown that the number of the frequency lines is directly proportional to the chirp factor. In order to achieve the highest number of frequency comb lines with the best flatness, the time delay between the driving voltages of the two MZMs is optimized. Our results reveal that at least 51 frequency lines can be observed at the output spectrum. In addition, 27 of these lines have power fluctuations of less than 1 dB. The performance of the proposed system is also simulated using a split-step numerical analysis. An optical frequency comb, with tunable frequency spacing ranging from 5 to 40 GHz, is successfully generated.

1. Introduction

Nowadays, optical frequency comb generator (OFCG) is widely used as multi-wavelength source for optical communication systems such as dense wavelength-division multiplexing (DWDM), optical time-division multiplexing, and optical orthogonal frequency-division multiplexing systems [1–6]. The generated comb is required to provide a stable frequency with a fixed phase and spacing for these applications. In addition, the flatness of spectral comb lines and low implementation costs are also vital requirements. Till today, many techniques have been proposed and developed to realize optical frequency combs (OFCs) such as the employment of a mode locked laser (MLL) [7,8]. The instability of carrier frequency due to the environment's dependency of laser cavity is the main disadvantage of MLL method [3]. Another technique is based on nonlinear effects in a highly nonlinear medium [9]. However, this technique requires a high power amplifier and an optical filter to shape the spectrum. Optical modulation technique can also be used to realize OFC whereby multiple optical carriers with precise channel spacing can be obtained from one seed light source [10–14]. Low cost, low complexity, small size, less noise [14], and high stability are some of the main advantages of this technique.

Many schemes have been used for generating OFCs such as by implementing optical modulation technique. This modulation is normally based on two approaches; amplitude-phase hybrid modulation and intensity modulation. In amplitude-phase hybrid modulation scheme, the number of generated comb lines is directly proportion to phase modulation (i.e. to tune the number of comb lines, the amplitude of electrical-oscillator signal is controlled) [10–12]. The limitations of this technique are mainly due to the limited number of generated comb lines and the use of high power of external RF to drive the modulators. Wu et. al. successfully demonstrated a 10 GHz comb with 38 lines within a spectral power variation of 1 dB by cascading intensity and phase modulations [11]. The problem of high power of external RF can be solved by employing optical intensity modulators with a low driving voltage. Shang et. al. used two cascaded intensity modulators to generate a 25 comb lines at low driving voltage [15].

In the optical intensity modulator, the change of phase of the output light with time causes a chirping in the optical signal. The

* Corresponding author at: Department of Electrical Engineering, Faculty of Engineering, University of Malaya, 50603 Kuala Lumpur, Malaysia.
E-mail address: swharun@um.edu.my (S.W. Harun).

http://dx.doi.org/10.1016/j.optcom.2015.01.054
0030-4018/

chirping allows the frequency of the optical signal to be increased (positive chirp) or decreased (negative chirp) during varying the driving signal. The chirping behavior of MZMs is often characterized by chirp factor [16]. The chirp factor is the intrinsic parameter to an optical modulator and depends on the device structures of optical modulators, such as the relation between the optical waveguides and the electrodes[17]. For producing high chirp factor, asymmetric MZM can be employed [18]. Most MZMs are fabricated with symmetric structure. They are manufactured for using as modulators with approximately zero-chirp factor. However, there are many techniques to control the chirping of symmetric MZMs. Changing the voltage biasing is easiest techniques to adjust the chirping of modulators where the chirp factor has been changed from -4 to 5 [19]. The chirp factor has also been controlled by introducing phase reversal electrode section in tandem with inverted ferroelectric domain section [20].

It is worth mentioning, in previous works, the amplitude and phase of driving voltages are tuned to generate a number of frequency lines while modulators have been assumed chirp-free modulators [11,21]. In this paper, a new technique to generate a flat and stable optical frequency comb is proposed based on employing MZMs with high chirp factors to reshape the modulated optical signal. The performance of the proposed technique is investigated for two different setups. The first setup employs only a single MZM, where electrical sinusoidal waveform is used to modulate the optical signal. The second setup uses two cascaded MZMs and a time delayer. This setup resembles the one proposed by Healy et. al. [22] where a dual-drive MZM is used. However the ideas behind the OFCG operation are different. In the work of Healy et. al., by adjusting the relative optical and RF phases of upper and lower interferometer arms, a non-flat but complementary optical spectra was obtained from phase modulation. However, a relatively flat optical frequency comb can be achieved by tuning and recombining the phases of the two arms. For the proposed setup, the first MZM is driven directly by a sinusoidal wave, while the second MZM is driven by a delayed replica of the sinusoidal wave. The time delay between the sinusoidal waves is used to reduce the power fluctuation in the generated optical comb spectrum. Specifically, we develop a mathematical model for both setups to prove the influence of the chirp factor on the number and flatness of generated frequency lines. The effect of MZM chirping on performance of both OFCGs is investigated using the mathematical analysis. Our mathematical model is validated by comparing the analytical results with simulation results obtained using the VPItransmissionMaker software.

The rest of the letter is organized as follows. In Section 2, the configurations of the proposed OFCG setups are introduced along with their mathematical models. Simulation results that provide the power spectra of the proposed OFCGs are presented in Section 3. Finally, the conclusion is given in Section 4.

2. System description and mathematical analysis

In this section, we introduce the configurations of the proposed OFCG setups. We also provide a simple mathematical model that best describes the proposed systems.

2.1. Single MZM configuration

We start our system description by providing an OFCG setup that is based on a single MZM.

Fig. 1 shows the configuration of this setup, which consists of a dual-electrode MZM, a CW laser source, and a periodic sinusoidal wave generator of period T. The schematic of a typical split (upper and lower) and dual electrode (separate DC and RF) configured Mach–Zehnder external modulator is shown in Fig. 1. This electrode configuration allows for separate control of both DC and RF modulating signals, as well as separate electro-optic control of both upper and lower arms of the MZM. The optical signals that pass through the arms of the MZM are chirped and their phases are simultaneously changed. Subsequently, the optical signals, which are obtained from two arms, are recombined to generate a relatively flat comb lines. In this setup, the optical CW laser is modulated by an electrical sinusoidal wave which is shifted by a DC voltage. Let the input optical field to the MZM be expressed as

$$E_i(t) = \sqrt{P_o}\,\exp\left(j2\pi f_o\right) \tag{1}$$

where P_o and f_o are the power and frequency of the input optical carrier, respectively. The corresponding output optical field can be written as [16,23]

$$E_o(t) = \frac{E_i(t)}{2}\left\{\exp\left(j\frac{(1+\alpha)\pi V_1(t)}{V_\pi}\right) + \exp\left(j\frac{(1-\alpha)\pi V_2(t)}{V_\pi}\right)\right\} \tag{2}$$

where $V_1(t)$ and $V_2(t)$ are the electrical driving signals supplied to both upper and lower MZM electrodes, respectively, α is a chirp factor and V_π is the voltage required to produce a 180° phase shift. In order to operate at a push–pull mode, the driven voltages of MZM are set $V_2(t) = -V_1(t)$. We assume that

$$V_1(t) = \frac{1}{2}\left\{V_{rf}\sin\left(\omega_r t\right) + V_{dc}\right\} \tag{3}$$

where V_{dc} is a DC voltage, V_{rf} is the amplitude of the sinusoidal wave, $\omega_r = 2\pi f_r$, and $f_r = 1/T$ is the frequency of the sinusoidal wave. Substituting in (2), we get

$$E_o(t) = \frac{E_i(t)}{2}\left\{\exp\left(j\frac{(1+\alpha)\pi\left(V_{rf}\sin\left(\omega_r t\right) + V_{dc}\right)}{2V_\pi}\right) + \exp\left(-j\frac{(1-\alpha)\pi\left(V_{rf}\sin\left(\omega_r t\right) + V_{dc}\right)}{2V_\pi}\right)\right\} \tag{4}$$

Then, the equation can be simplified as

$$E_o(t) = \frac{E_i(t)}{2}\{\exp\left[jA_2\sin\left(\omega_r t\right)\right]\exp\left(jA_1\right) + \exp\left[-jA_4\sin\left(\omega_r t\right)\right]\exp\left(-jA_3\right)\} \tag{5}$$

where;

$$A_1 = \frac{\pi(1+\alpha)}{2V_\pi}V_{dc},$$

$$A_2 = \frac{\pi(1+\alpha)}{2V_\pi}V_{rf},$$

$$A_3 = \frac{\pi(1-\alpha)}{2V_\pi}V_{dc},\ \text{and}$$

$$A_4 = \frac{\pi(1-\alpha)}{2V_\pi}V_{rf}.$$

For achieving modulation in intensity, the MZM should be operated at the quadrature point, where a DC bias is $V_\pi/2$ and a peak-to-peak modulation is V_π. Then V_{rf}, which represents the peak of RF signal should be equal to $V_\pi/2$. This mode of operation allows the output optical signal to increase and decrease around the operating point of MZM without distortion as the RF signal swings through a complete cycle. Assuming that $V_{rf} = V_{dc} = V_\pi/2$, we have $A_1 = A_2$ and $A_3 = A_4 = \pi/2 - A_1$. Substituting A_2, A_3 and A_4 in terms of A_1 in (5), we get

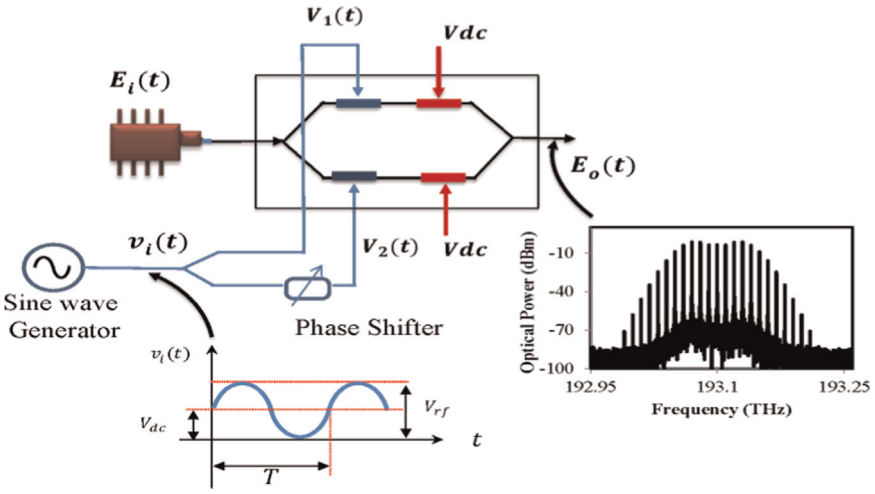

Fig. 1. Configuration of an optical frequency comb generator using a single MZM.

$$E_o(t) = \frac{E_i(t)}{2}\exp(jA_1)\left\{\exp[jA_1\sin(\omega_r t)] - j\exp\left[-j\left(\frac{\pi}{2} - A_1\right)\sin(\omega_r t)\right]\right\} \quad (6)$$

Finally, the equation can be expressed using the Bessel functions as follows:

$$E_o(t) = \frac{\sqrt{P_o}\exp(jA_1)}{2}\left\{\left[J_0(A_1) - jJ_0\left(A_1 - \frac{\pi}{2}\right)\right]\exp(j2\pi f_o t) + \sum_{\substack{n=-\infty \\ n\neq 0}}^{\infty} J_n(A_1)\exp\left(j2\pi\left(f_o + nf_r\right)t\right) - j\sum_{\substack{n=-\infty \\ n\neq 0}}^{\infty} J_n\left(A_1 - \frac{\pi}{2}\right)\exp\left(j2\pi\left(f_o + nf_r\right)t\right)\right\} \quad (7)$$

The first term in (7) represents the center frequency line of the OFCG, while the second and third terms create the rest of the comb lines. As it is shown from (7), the number of comb lines is determined by A_1. That is, the number of comb lines is controlled by the chirp factor α when both V_{rf} and V_{dc} are set to a constant value. Additionally, the spacing between the comb lines is governed by the oscillation frequency f_r.

2.2. Two cascaded MZMs configuration

Based on (7), in order to increase the number of comb lines, the optical pulse has to be reshaped. In this subsection, we introduce a two-cascaded MZMs configuration in order to reshape the pulse optically.

Fig. 2 shows the corresponding setup, which consists of a CW laser diode, a time delayer, a sinusoidal wave oscillator, and two MZMs. The laser diode generates a CW light with electric field $E_i(t)$ as given in (1). The first MZM is driven directly by a sinusoidal wave oscillator with frequency f_r, while the second MZM is driven by same sinusoidal wave after being delayed by a certain time delay δ, satisfying the condition $0 < \delta < 0.5$ T. The output fields of the first and second MZMs are given by

$$\begin{aligned} E_{o1}(t) &= \frac{E_i(t)}{2}\{\exp[jA_2\sin(\omega_r t)]\exp(jA_1) + \exp[-jA_4\sin(\omega_r t)]\exp(-jA_3)\}, \\ E_o(t) &= \frac{E_i(t)}{2}\{\exp[jA_2\sin(\omega_r(t-\delta))]\exp(jA_1) + \exp[-jA_4\sin(\omega_r(t-\delta))]\exp(-jA_3)\}, \end{aligned} \quad (8)$$

respectively. Similar to last section, we employ the condition $V_{rf} = V_{dc} = V_\pi/2$. Again adopting Bessel functions, the optical field of the OFCG can be expressed as

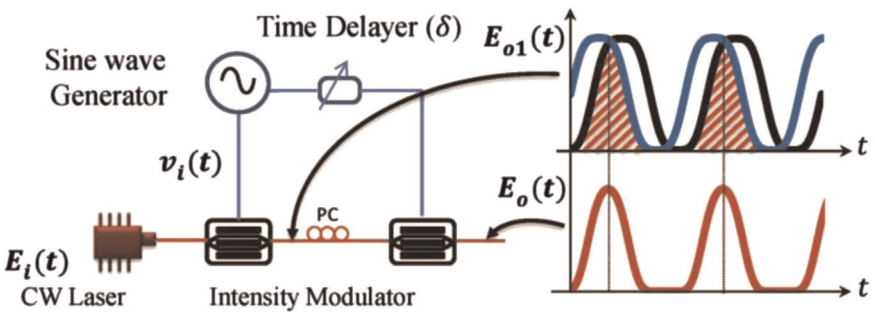

Fig. 2. Configuration of an optical frequency comb generator using two cascaded MZMs.

$$E_o(t) = \frac{E_i(t)\exp(j2A_1)}{4}\left[\sum_{n=-\infty}^{\infty} J_n(A_1)\exp(jn\omega_r t) - j\sum_{n=-\infty}^{\infty} J_n\left(A_1-\frac{\pi}{2}\right)\exp(jn\omega_r t)\right] \times \left[\sum_{n=-\infty}^{\infty} J_n(A_1)\exp(jn\omega_r(t-\delta)) - j\sum_{n=-\infty}^{\infty} J_n\left(A_1-\frac{\pi}{2}\right)\exp(jn\omega_r(t-\delta))\right] \quad (9)$$

3. Results and discussion

In this section, we present a simulation result of our proposed systems, which was obtained using the VPItransmissionMaker commercial software. The simulated results are also compared with theoretical results obtained from the mathematical analysis developed in the last section for comparison purpose. Moreover, our proposed systems are tested by changing the chirp factor from 3 to 9. Because the highest value of chirp factor has been experimentally measured at $\alpha=5$ [19], most results of our paper are obtained at $\alpha=5$.

3.1. Simulation results of single MZM configuration

The single-MZM comb generator described in Fig. 1 has been simulated and the resulting optical spectra are depicted in Figs. 3 and 4. In our setup, a 10 dBm CW optical carrier is generated by a laser diode with a frequency of 193.1 THz and a linewidth of 100 kHz. The driven voltages of MZM are adjusted to $V_{rf} = V_{dc} = V_\pi/2$.

In Fig. 3, we plot the optical spectra of a single-MZM comb generator with a constant chirp factor $\alpha=5$ for different oscillation frequencies varying from 5 GHz to 40 GHz. Fig. 3(a) shows the output spectrum with oscillation frequency of 5 GHz, where it can be seen that 23 comb lines can be generated. The frequency spacing between the lines is 5 GHz, while the bandwidth is 115 GHz. As expected, as an oscillation frequency is increased to 10 GHz, the number of comb lines remains constant, but the frequency spacing between the lines is increased to 10 GHz and the bandwidth is doubled as shown in Fig. 3(b). Similarly, by increasing the oscillation frequency even further, the number of comb lines remains constant, but both the frequency spacing and bandwidth are increased accordingly, as depicted in Fig. 3(c) and (d). Fig. 4 shows the relation between the number of frequency lines and the chirp factor, where the optical spectra for chirp factors of 3, 5, 7, and 9 are depicted in the figure. The oscillation frequency is set constant at $f_r=10$ GHz. It can be seen from the figure that comb lines counts of 19, 23, 29, and 33 are achieved when the chirp factor is set to 3, 5, 7, and 9, respectively. The simulation results show that the number of frequency lines in the optical comb generator is broadly tunable by changing the chirp factor, which agrees with the mathematical analysis of the output optical field $E_o(t)$ obtained in (7).

3.2. Simulation results of two-cascaded MZMs configuration

The cascaded-MZMs OFCG of Fig. 2 is simulated with input CW light of frequency $f_o=193.1$ THz and optical power of 10 dBm. The oscillation frequency is set fixed at $f_r=10$ GHz, while the amplitude and biasing of the input sinusoidal wave are selected so that $v_i(t) = 0.5\left[V_\pi \sin(2\pi f_r t) + V_\pi\right]$. Furthermore, the time delay δ is

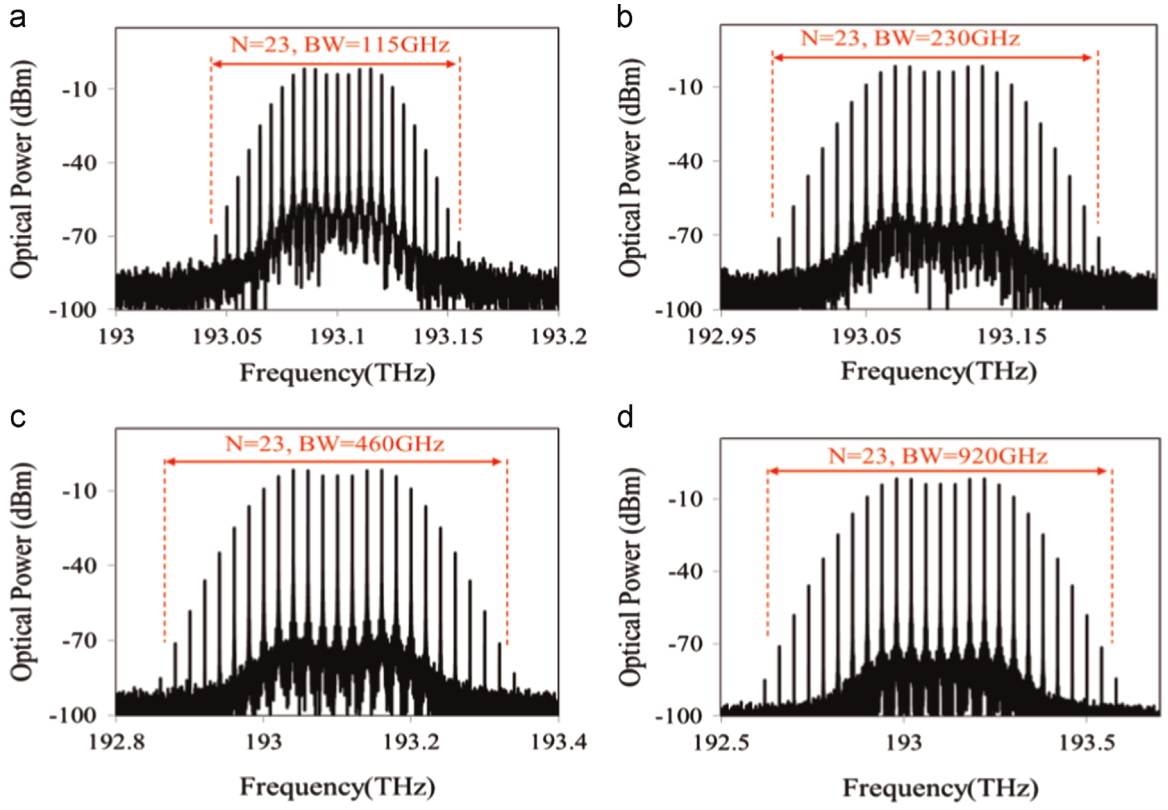

Fig. 3. Optical spectra of a single-MZM comb generator with a constant chirp factor $\alpha=5$ for different oscillation frequencies: (a) $f_r=5$ GHz, (b) $f_r=10$ GHz, (c) $f_r=20$ GHz and (d) $f_r=40$ GHz.

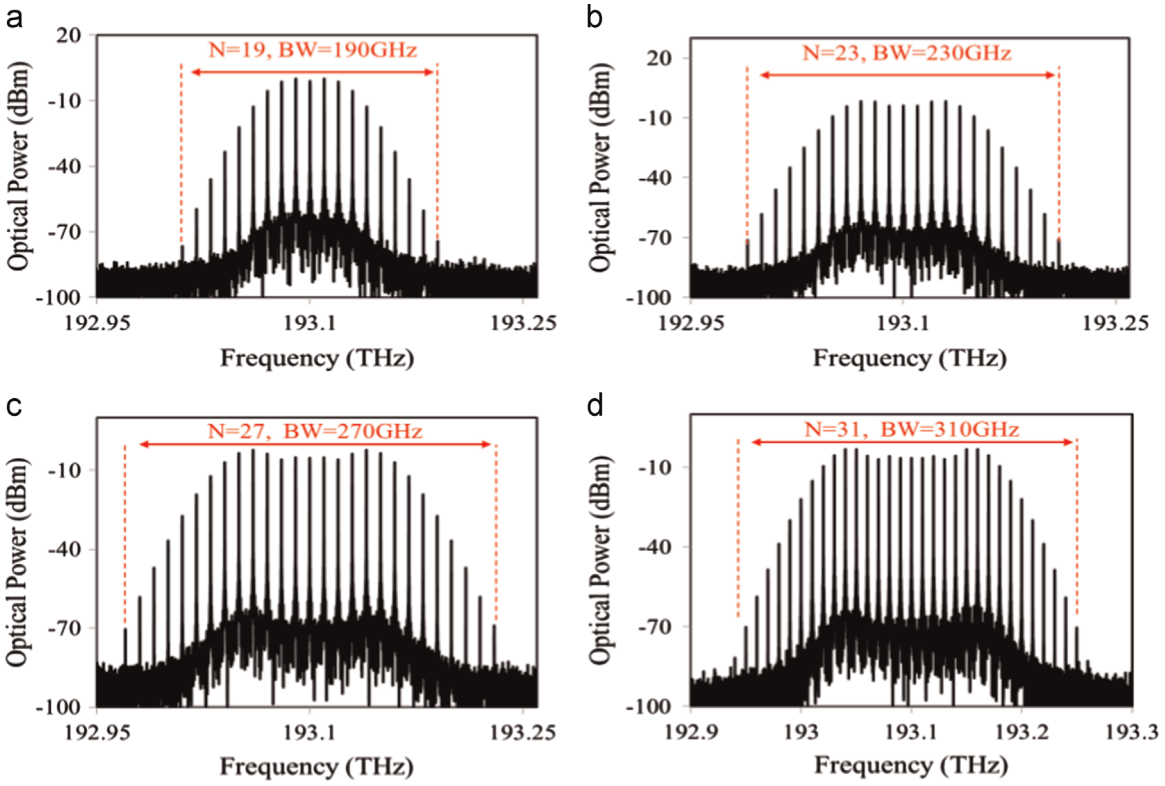

Fig. 4. Optical spectra of a single-MZM comb generator with a constant $f_r=10$ GHz for different chirp factors: (a) $\alpha=3$, (b) $\alpha=5$, (c) $\alpha=7$ and (d) $\alpha=9$.

adjusted to zero and the chirp factors for both MZMs are assumed to be identical and take values in the set$\alpha \in \{3, 5, 7, 9\}$. The optical spectra obtained by the simulation are shown in Fig. 5. It can be seen from Fig. 5(a) that using a chirp factor $\alpha=3$, the proposed OFCG setup generates an optical power spectrum with 23 comb lines. Increasing α to 5, 7, and 9, yields 35, 43, and 51 comb lines in

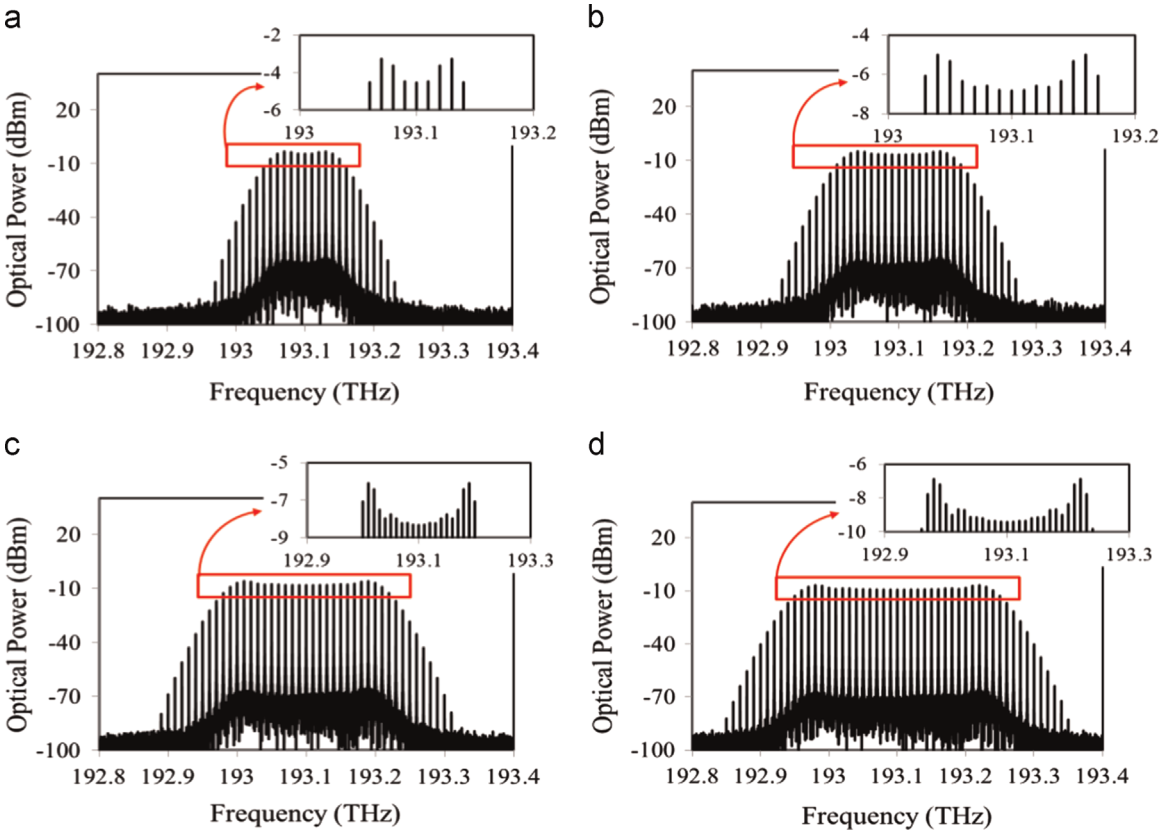

Fig. 5. Optical spectra of a cascaded-MZMs comb generator with $f_r=10$ GHz and $\delta=0$ for different chirp factors: (a) $\alpha=3$, (b) $\alpha=5$, (c) $\alpha=7$ and (d) $\alpha=9$.

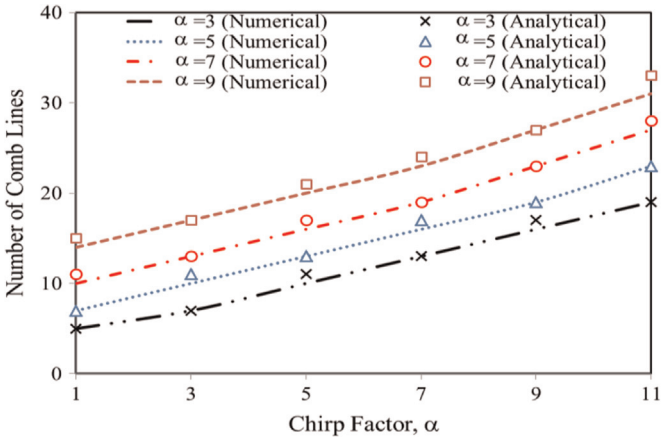

Fig. 6. Number of frequency lines versus chirp factor of second MZM at various values for chirp factors of first MZM.

3.2.1. Optimizing the flatness

In order to improve the flatness of optical spectrum, the input wave amplitude, biasing and time delay should be optimized. For example, let the amplitude and biasing of the input wave be set so that $v_i(t)=0.5V_\pi \sin(2\pi f_r t)+0.4V_\pi$ and the time delay is varied from 0 to 0.2 T, while the chirp factor for both MZMs is fixed at 5. The DC value of $0.4V_\pi$ achieves the lowest power fluctuation and it is obtained by varying Vdc using the VPI software. The corresponding optical spectra are shown in Fig. 7. By adjusting $\delta=0$, the 0.9 dB power fluctuation can be obtained from Fig. 7(a). Increasing δ to 0.1 T, 0.15 T, and 0.2 T, produces 0.55, 0.45, and 0.7 dB power fluctuation in the optical spectra, respectively. That is, lower power fluctuation is observed in the optical spectrum at time delay of 15% of wave period where the two MZMs are operating in optimum condition, Fig. 7(c).

In order to explore more the effect of delay time on flatness of optical combs, the optical power fluctuation versus delay time is

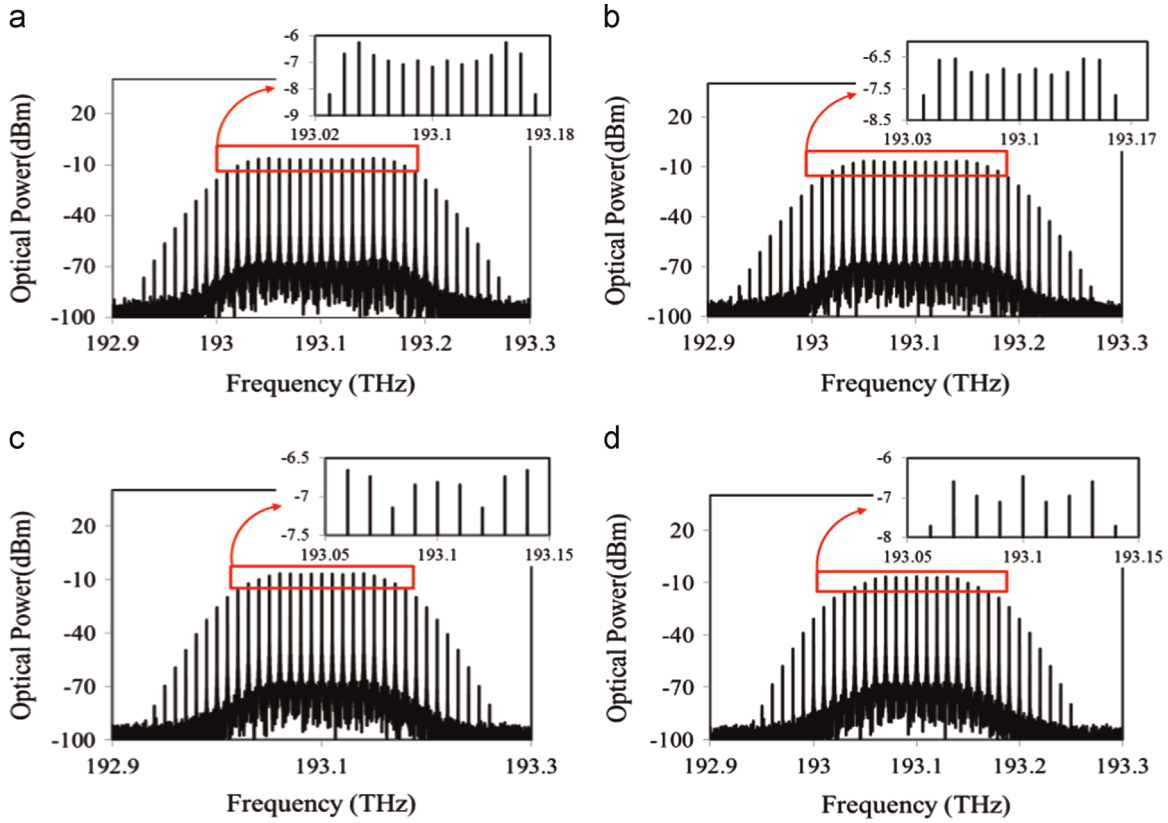

Fig. 7. Optical spectra of a cascaded-MZMs comb generator at a constant $f_r=10$ GHz and $\alpha=5$ for different delay times: (a) $\delta=0$, (b) $\delta=0.1$ T, (c) $\delta=0.15$ T and (d) $\delta=0.2$ T.

the optical spectra, respectively. This shows that, increasing the chirp factor would increase both the number of comb lines and fluctuation. This phenomenon results from the multiplication of a lot of sinusoidal waveforms. In agreement with (9), a higher value of chirp factor leads to more harmonic frequencies and wider optical spectra.

Fig. 6 depicts the number of frequency lines with fluctuation power of less than 1 dB as a function of chirp factor α. In order to have insight of presented system setup, the chirp factor of second MZM in the cascaded setup is varied from 1 to 11 while the first MZM is fixed at 3, 5, 7, and 9. The highest frequency comb lines are achieved at highest value of chirp factors. The corresponding values from analytical results are also indicated in the same figure, which shows good agreement with simulation results.

plotted in Fig. 8. In agreement with Fig. 7, the minimum fluctuation is achieved at $\delta=0.15$ T for all chirp factor values of 5, 7, and 9. In addition, the effect of delay timer on number of frequency lines is also demonstrated in Fig. 8. As it can be seen, the number of frequency lines is related inversely to delay time. For the sake of convenience, in Fig. 9 we plot the optical power fluctuation and number of frequency lines versus delay time for the case when $V_{dc}=0.5V_\pi$. It can be noticed that at $\delta=0$, although the number of comb lines are higher than that of the previous case of $V_{dc}=0.4V_\pi$, the corresponding power fluctuations are also higher. It is also seen that the points of minimum power fluctuations occur at a fixed point of 0.2 T. From the last two figures, we have the following observations at the points of minimum power fluctuations. At $\alpha=5$, the number of comb lines is 9 for both cases of $V_{dc}=0.4V_\pi$ and $V_{dc}=0.5V_\pi$. However, the corresponding power fluctuations

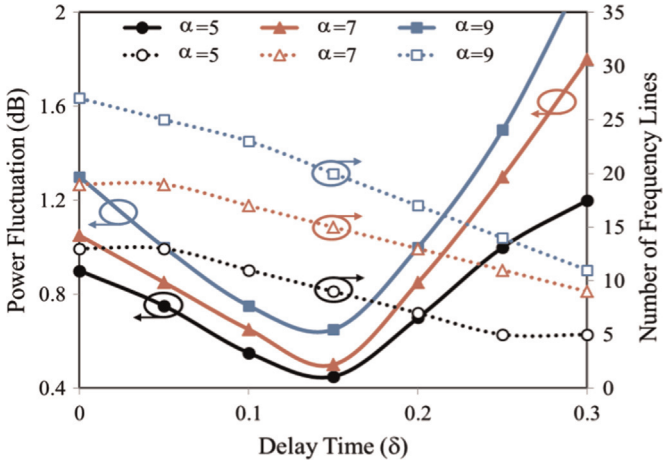

Fig. 8. Power fluctuation and number of frequency lines versus delay time δ at $V_{dc}=0.4V_{\pi}$ for various chirp factors.

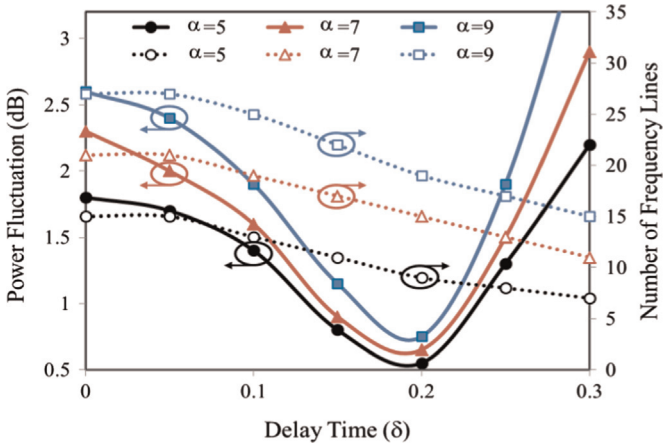

Fig. 9. Power fluctuation and number of frequency lines versus delay time δ at $V_{dc}=0.5V_{\pi}$ for various chirp factors.

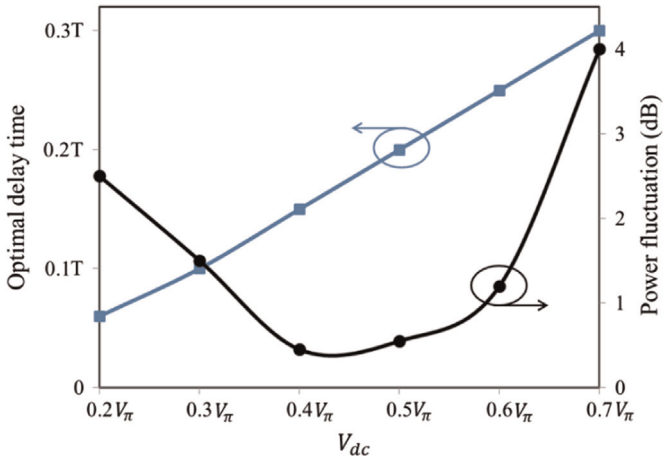

Fig. 10. The optimal delay time and power fluctuation as a function of Vdc at chirp factor of $\alpha=5$.

are 0.45 dB and 0.55 dB, respectively. Also, for $\alpha=7$, the number of comb lines is 15 for both cases of $V_{dc}=0.4V_{\pi}$ and $V_{dc}=0.5V_{\pi}$, and the corresponding fluctuations are 0.5 dB and 0.65 dB, respectively. Moreover, for $\alpha=9$, the number of comb lines is 21 with power fluctuations of 0.65 dB for the case of $V_{dc}=0.4V_{\pi}$, while the number of comb lines is 19 with power fluctuations of 0.75 dB for the other case of $V_{dc}=0.5V_{\pi}$. Furthermore, it is seen that the effect of time delay on the power fluctuation is higher for suboptimum scenarios. For example, in Fig. 9 with $\alpha=5$, the fluctuation is changed from 1.8 to 0.55 dB when δ is varied from 0 to 0.2 T, while, in Fig. 8 with same chirp factor, the fluctuation is changed from 0.9 to 0.45 dB only when δ is varied from 0 to 0.15 T. Fig. 10 shows both the optimal delay time and fluctuation as a function of V_{dc} at chirp factor of $\alpha=5$. The optimal delay time increases linearly with the increment of the biasing voltage. Conversely, the fluctuation grows in magnitude when the biasing voltage is lower or greater than $0.4V_{\pi}$.

4. Conclusion

A new approach for generating an optical frequency comb based on chirping of two cascaded MZMs has been proposed. The MZMs are driven by a sinusoidal wave oscillator and its delayed replica in order to produce periodic optical pulses. A broadband optical spectrum with a large number of frequency lines and good flatness has been achieved in the proposed setup. It has been seen that the flatness of optical spectra is improved by adjusting the delay time between the driven voltages of two MZM. The bandwidth of the optical comb signal is determined by the frequency of the sinusoidal wave, the chirp factor, and the time delay. Our results reveal that more than 35 frequency lines can be obtained at a chirp factor of 5. Furthermore, 13 comb lines can be achieved with power variation of less than 1 dB. The results showed the considerable approach for generation OFCGs.

References

[1] Z. Jiang, D.E. Leaird, C.-B. Huang, H. Miao, M. Kourogi, K. Imai, A.M. Weiner, Spectral line-by-line pulse shaping on an optical frequency comb generator, IEEE J. Quantum Electron. 43 (2007) 1163–1174.
[2] H.-J. Song, N. Shimizu, T. Furuta, K. Suizu, H. Ito, T. Nagatsuma, Broadband-frequency-tunable sub-terahertz wave generation using an optical comb, AWGs, optical switches, and a uni-traveling carrier photodiode for spectroscopic applications, J. Lightw. Technol. 26 (2008) 2521–2530.
[3] I. Morohashi, T. Sakamoto, H. Sotobayashi, T. Kawanishi, I. Hosako, Broadband optical comb generation using Mach–Zehnder-modulator-based flat comb generator with feedback loop, in: Proceedings of the 36th European Conference and Exhibition on Optical Communication (ECOC), IEEE, 2010, pp. 1–3.
[4] S.E. Mirnia, A. Zarei, S.D. Emami, S.W. Harun, H. Arof, H. Ahmad, H.M. Shalaby, Proposal and performance evaluation of an efficient RZ-DQPSK modulation scheme in all-optical OFDM transmission systems, J. Opt. Commun. Netw. 5 (2013) 932–944.
[5] B.J. Chun, S. Hyun, S. Kim, S.-W. Kim, Y.-J. Kim, Frequency-comb-referenced multi-channel fiber laser for DWDM communication, Opt. Express 21 (2013) 29179–29185.
[6] C. Chen, C. Zhang, W. Zhang, W. Jin, K. Qiu, Scalable and reconfigurable generation of flat optical comb for WDM-based next-generation broadband optical access networks, Opt. Commun. 321 (2014) 16–22.
[7] E. Benkler, F. Rohde, H.R. Telle, Endless frequency shifting of optical frequency comb lines, Opt. Express. 21 (2013) 5793–5802.
[8] Y.-J. Kim, J. Jin, Y. Kim, S. Hyun, S.-W. Kim, A wide-range optical frequency generator based on the frequency comb of a femtosecond laser, Opt. Express. 16 (2008) 258–264.
[9] X. Yang, D.J. Richardson, P. Petropoulos, Broadband, flat frequency comb generated using pulse shaping-assisted nonlinear spectral broadening, IEEE Photon. Technol. Lett. 25 (2013) 543–545.
[10] V. Torres-Company, A.M. Weiner, Optical frequency comb technology for ultra-broadband radio-frequency photonics, Laser Photon. Rev. 8 (2014) 368–393.
[11] R. Wu, V. Supradeepa, C.M. Long, D.E. Leaird, A.M. Weiner, Generation of very flat optical frequency combs from continuous-wave lasers using cascaded intensity and phase modulators driven by tailored radio frequency waveforms, Opt. Lett. 35 (2010) 3234–3236.
[12] C. Chen, C. Zhang, D. Liu, K. Qiu, S. Liu, Tunable optical frequency comb enabled scalable and cost-effective multiuser orthogonal frequency-division multiple access passive optical network with source-free optical network units, Opt. Lett. 37 (2012) 3954–3956.
[13] L. Shang, A. Wen, G. Lin, Y. Gao, A flat and broadband optical frequency comb with tunable bandwidth and frequency spacing, Opt. Commun. 331 (2014) 262–266.
[14] M. Wang, X. Zhang, Tunable Optical Frequency Comb Generation Based on an

Optoelectronic Oscillator, IEEE Photon. Technol. Lett. 25 (2013) 2035–2038.
[15] L. Shang, A. Wen, G. Lin, Optical frequency comb generation using two cascaded intensity modulators, J. Opt. 16 (2014) 035401.
[16] F. Koyama, K. Iga, Frequency chirping in external modulators, J. Lightw. Technol. 6 (1988) 87–93.
[17] S. Oikawa, T. Kawanishi, M. Izutsu, Measurement of chirp parameters and halfwave voltages of Mach–Zehnder-type optical modulators by using a small signal operation, IEEE Photon. Technol. Lett. 15 (2003) 682–684.
[18] J. Nayyer, H. Nagata, S. Shimotsu, S. Oikawa, M. Yamada, Modulation characteristics of high-speed optical modulators with properly split asymmetry into their Mach-Zehnder arms, Electron. Lett. 31 (1995) 387–388.
[19] M. Schiess, H. Carlden, Evaluation of the chirp parameter of a Mach–Zehnder intensity modulator, Electron. Lett. 30 (1994) 1524–1525.
[20] N. Courjal, H. Porte, A. Martinez, J.-P. Goedgebuer, $LiNbO_3$ Mach–Zehnder modulator with chirp adjusted by ferroelectric domain inversion, IEEE Photon. Technol. Lett. 14 (2002) 1509–1511.
[21] T. Sakamoto, T. Kawanishi, M. Izutsu, Asymptotic formalism for ultraflat optical frequency comb generation using a Mach–Zehnder modulator, Opt. Lett. 32 (2007) 1515–1517.
[22] T. Healy, F.C. Garcia Gunning, A.D. Ellis, J.D. Bull, Multi-wavelength source using low drive-voltage amplitude modulators for optical communications, Opt. Express. 15 (2007) 2981–2986.
[23] K.-P. Ho, J.M. Kahn, Spectrum of externally modulated optical signals, J. Lightw. Technol. 22 (2004) 658.